

SPECTRAL APPROACH TO KORTEWEG-DE VRIES EQUATIONS ON THE COMPACTIFIED REAL LINE

CHRISTIAN KLEIN AND NIKOLA STOILOV

ABSTRACT. We present a numerical approach for generalised Korteweg-de Vries (KdV) equations on the real line. In the spatial dimension we compactify the real line and apply a Chebyshev collocation method. The time integration is performed with an implicit Runge-Kutta method of fourth order. Several examples are discussed: initial data bounded but not vanishing at infinity as well as data not satisfying the Faddeev condition, i.e. with a slow decay towards infinity.

1. INTRODUCTION

Generalised Korteweg-de Vries (gKdV) equations,

$$(1) \quad u_t(x, t) + u_{xxx}(x, t) + u(x, t)^{p-1}u_x(x, t) = 0,$$

where $p \in \mathbb{N}$, $u : \mathbb{R} \times \mathbb{R}^+ \mapsto \mathbb{R}$, appear as asymptotic models in hydrodynamics, nonlinear optics, plasma physics, Bose-Einstein condensates, and essentially in most situations where predominantly one-dimensional phenomena are discussed and where dispersion dominates dissipation. Whereas this applies in particular to the case of the classical Korteweg-de Vries (KdV) equation ($p = 2$), there are applications for instance in electrodynamics for the modified KdV equation ($p = 3$), see [21]. Because of their importance in applications, there has been a considerable activity in developing numerical approaches for the gKdV equations. For initial data which are periodic or rapidly decreasing, numerical approaches based on the approximation of u in (1) via truncated Fourier series, i.e., trigonometric polynomials, are very efficient, see for instance [14, 15] and references therein.

The Fourier approach, that is restricting the data to an interval $L[-\pi, \pi]$ ($L = \text{const}$, $L \in \mathbb{R}^+$) and continuing them periodically with period $2\pi L$ on the whole real line works very well for periodic functions and exhibits *spectral convergence*, namely an exponential decrease of the numerical error with the number of Fourier modes. Schwartz class functions can be treated as periodic as one works with a finite precision and since L can be chosen large enough such that all necessary derivatives of u vanish at the domain boundaries with numerical precision. However, the same approach for initial data which do not tend to zero or are only slowly decreasing to zero for $x \rightarrow \infty$, would in general imply a Gibbs phenomenon at the domain boundaries. The resulting method would therefore be only of first order in the number of Fourier modes, making it impossible to reach the high resolution

Date: December 21, 2021.

This work is partially supported by the ANR-FWF project ANuI - ANR-17-CE40-0035, the isite BFC project NAANoD, the ANR-17-EURE-0002 EIPHI and by the European Union Horizon 2020 research and innovation program under the Marie Skłodowska-Curie RISE 2017 grant agreement no. 778010 IPaDEGAN.

necessary to treat e.g. rapid oscillations in the solution. Therefore, such situations are typically treated on a finite interval. This leads to the problem of how to impose boundary conditions, so that inside the computational domain the solution is the same as if the computation was done on the whole real line. Such boundary conditions are called *transparent*. Bérenger [2] introduced *perfectly matched layers* (PML) in electrodynamics to address this problem by extending the computational domain to layers glued to the domain boundaries. Inside the layers, the equation under consideration is deformed to a dissipative one, which is chosen to efficiently dissipate the solution. Whereas this works well for linear equations, examples for the nonlinear Schrödinger equation, see [26, 3], showed that in a nonlinear setting there will be back reflections from the layers to the computational domain. For integrable equations exact transparent boundary conditions (TBC) can be given, e.g. for the case of modified KdV see [27] based on [9]. The problem with both PML and TBC is that they in general require initial data with compact support within the computational domain, thus limiting the class of solutions that can be studied. The goal of the present paper is to establish a spectral numerical approach for generalised KdV equations (1) for initial data that are analytic on the whole real line, that are slowly decreasing towards infinity, or are bounded there. This numerical approach exhibits spectral convergence on the whole real line with a technique similar to [12].

Both the classical KdV equation and the modified KdV equation are completely integrable, which means they have an infinite number of conserved quantities (for a comprehensive review on integrability see [25]). In all other cases, the generalised KdV equations have only three conserved quantities, $\int_{\mathbb{R}} u dx$ and the L^2 norm of u and the energy

$$(2) \quad E[u] = \int_{\mathbb{R}} \left(\frac{u^{p+1}}{p(p+1)} - \frac{1}{2} u_x^2 \right) dx.$$

The complete integrability of the classical KdV equation made it one of the best studied non-linear dispersive equations with a rather complete understanding of its solutions. However, even in this case there are open questions which motivate us to provide numerical tools to complement analytical studies in this context. The standard inverse scattering approach to KdV is only applicable if the Faddeev decay condition [8],

$$(3) \quad \int_{\mathbb{R}} (1 + |x|) |u_0(x)| dx < \infty,$$

holds for the initial data $u(x, 0) = u_0(x)$. The direct scattering approach to KdV involves the determination of the spectrum of the Schrödinger equation for the potential $u_0(x)$,

$$\psi_{xx} + u_0(x)\psi = E\psi,$$

see [25]. It is known that this discrete spectrum is finite if the Faddeev condition (3) is satisfied, see [17]. But except for the periodic case, see for instance [1], there is no complete understanding of the case of initial data not satisfying (3). The goal of the present paper is to provide numerical tools to study such cases. Of course, numerically one will be only able to study finite times and thus will not be able to address the question whether the time evolution of such data can lead to an infinite number of solitons.

The paper is organized as follows: In section 2 we summarize a few theoretical facts on generalised KdV equations. In section 3 we choose a compactification of the real line and describe the numerical approach for the generalised KdV equations. In section 4 we discuss several examples. Concluding remarks are added in section 5.

2. THEORETICAL PRELIMINARIES

In this section we summarize basic facts about generalised KdV equations needed in the following.

Though the KdV equations (1) are only completely integrable for $p = 2$ and $p = 3$, they have for all integer values of $p \geq 2$ a solitary travelling wave solution which is explicitly given by $u = Q_c(x - x_0 - ct)$ with $x_0, c = \text{const}$ and with

$$(4) \quad Q_c(z) = \left(\frac{p(p+1)c}{2} \operatorname{sech}^2 \frac{\sqrt{c}(p-1)}{2} z \right)^{1/(p-1)}.$$

Thus, we have $Q_c(z) = c^{1/(p-1)} Q(\sqrt{c}z)$, where we have put $Q := Q_1$. This simple scaling property of the *solitons* allows to concentrate on the case $c = 1$. If we refer in the following to the generalised KdV soliton, it is always implied that $c = 1$. It was shown in [4] that these solitons are linearly unstable for $p > 4$. Note that the energy of the soliton vanishes for $p = 5$.

The generalised KdV equation has the following scaling invariance: $x \mapsto x/\lambda$, $t \mapsto t/\lambda^3$ and $u \mapsto \lambda^{2/(p-1)}u$ with $\lambda = \text{const}$. For $p = 5$, the L^2 norm of u is invariant under this rescaling, and this case is consequently called L^2 -critical. It is shown in [18] that solutions to the L^2 critical generalised KdV equation can have a blow-up in finite time for smooth initial data. The mechanism of the blow-up for initial data close to the soliton is discussed in [20]. In the present paper, we will only study the sub-critical cases, $p \leq 4$.

A convenient way to treat solutions varying on length scales of order $1/\epsilon$ for times of order $1/\epsilon$ for $0 < \epsilon \ll 1$ is to consider the map $x \mapsto \epsilon x$, $t \mapsto \epsilon t$. This leads for (1) to (once more we use the same symbol u for the transformed and the original solution)

$$(5) \quad u_t + \epsilon^2 u_{xxx} + u^{p-1} u_x = 0.$$

The formal limit $\epsilon \rightarrow 0$ of this equation yields a generalised Hopf equation, $u_t + u^{p-1} u_x = 0$. It is known that such equations can have a *hyperbolic blow-up*, i.e., shocks for general smooth initial data, for instance for data with a single hump. The generic *break-up* of such solutions at a point (x_c, t_c, u_c) , see for instance the discussion in [7] and references therein, is characterized by the equations

$$(6) \quad \begin{aligned} a(u_c)t_c + \Phi(u_c) &= x_c, \\ a'(u_c)t_c + \Phi'(u_c) &= 0, \\ a''(u_c)t_c + \Phi''(u_c) &= 0, \end{aligned}$$

where $a(u) = u^{p-1}$. It is known that dispersive regularizations of dispersionless equations as (5) in our case will lead to *dispersive shock waves* (DSWs), i.e., rapid modulated oscillations near the shock of the solution of the corresponding dispersionless equation for the same initial data. Dubrovin [5, 6] presented a conjecture that the onset of a DSW is *universal* for a large class of dispersive equations and of initial data, and that it is given by a special solution of the so-called Painlevé P_I^2

equation, see for instance [11]. This conjecture was numerically shown to apply to the generalised KdV equations in [7]. In this paper we provide the numerical tools to do so for larger classes of initial data than in [7], however we leave addressing the universality conjecture in the present context for a future work.

3. NUMERICAL APPROACH

In this section we present the numerical approach to treat generalised KdV equations on the compactified real line. We first introduce the compactification which allows to study the equation on the interval $[-1, 1]$ where we use a Chebyshev collocation method. The resulting system of ordinary differential equations is then integrated in time with an implicit Runge-Kutta scheme.

3.1. Compactification. To numerically treat the KdV equation, we first map the real line via the well known map (this is the standard compactification used for Minkowski spacetime)

$$(7) \quad x = c \tan \frac{\pi l}{2}, \quad l \in [-1, 1], \quad c = \text{const},$$

to the interval $[-1, 1]$. This implies

$$(8) \quad \partial_x = \frac{2}{\pi c} \cos^2 \frac{l\pi}{2} \partial_l.$$

The role of the constant c is to control the numerical resolution in various parts of the real line within certain limits. This is illustrated in Fig. 1 where we have introduced *Chebyshev collocation points* for $l \in [-1, 1]$, i.e.,

$$(9) \quad l_n = \cos(n\pi/N), \quad n = 0, 1, \dots, N, \quad N \in \mathbb{N}.$$

It can be seen in Fig. 1 that the density of the points near $x = 0$ is higher for smaller c (numerically the function \tilde{v} is studied as a function of l , but since in applications the dependence on x is more important, we plot its x -dependence which can be obtained via (7)). Note, however, that the spectral methods we apply in this paper are global. This means that a high resolution in part of the studied domain is not necessarily beneficial, only the overall resolution on the whole interval is important. Therefore we generally apply values of c close to 1.

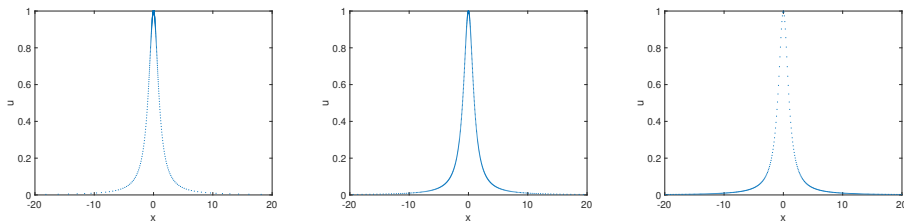


FIGURE 1. Distribution of the Chebyshev collocation points (9) on a Lorentzian profile under the map (7) for $N = 800$; on the left for $c = 0.1$, in the middle for $c = 1$, on the right for $c = 10$.

3.2. Boundary conditions. The map (7) transforms the KdV equation (1) on the real line to an equation on the interval $[-1, 1]$, which is singular at the points $l = \pm 1$. Because of this singular behavior, no boundary conditions need to be imposed there. However, in practice it is useful to give boundary conditions at these points to stabilize the numerical approaches. We apply a vanishing condition for u at these points, and a *clamped boundary condition* for $l = -1$, i.e., the three conditions (in an abuse of notation, we denote $u(x, t)$ and $u(l, t)$ with the same letter)

$$(10) \quad u(l, t) \Big|_{l=1} = 0, \quad u(l, t) \Big|_{l=-1} = 0, \quad u_l(l, t) \Big|_{l=-1} = 0.$$

The approach we present here can be generalised to functions u which do not tend to 0 for $|x| \rightarrow \infty$, but which are bounded there. In this case we write

$$(11) \quad u = v + V, \quad V = A \frac{1+l}{2} + B \frac{(1+l)^2}{4} + C \frac{1-l}{2},$$

where A, B, C are constants such that $v(l = \pm 1) = v_l(l = -1) = 0$. To treat the clamped boundary condition for $l = -1$, we use as in [22] the ansatz

$$(12) \quad v = (1+l)\tilde{v}.$$

This leads for (1) to the equation

$$(13) \quad \tilde{v}_t + \frac{1}{1+l}[(1+l)\tilde{v} + V]_{xxx} + \frac{1}{1+l}[(1+l)\tilde{v} + V]^p[(1+l)\tilde{v} + V]_x = 0$$

which has to be solved for all t with the condition $\tilde{v}(\pm 1) = 0$.

3.3. Chebyshev differentiation matrices. The dependence of \tilde{v} in (13) on l will be treated in standard way via Lagrange interpolation of \tilde{v} on Chebyshev collocation points (9) as discussed in [22]. A derivative of \tilde{v} with respect to l is then approximated via the derivative of the Lagrange polynomial. This leads to the action of a matrix on the vector $\tilde{v} = (\tilde{v}(l_0), \dots, \tilde{v}(l_N))$ (again we use the same symbol for the function \tilde{v} and the vector \tilde{v}), the well known *Chebyshev differentiation matrices* D , see e.g., [23, 24]. This means with (8) that the derivatives ∂_x are approximated by

$$(14) \quad \partial_x \approx \frac{2}{\pi c} \text{diag} \left(\cos^2 \frac{l\pi}{2} \right) D,$$

where the diagonal matrix has the components $(\cos^2 \frac{l_0\pi}{2}, \dots, \cos^2 \frac{l_N\pi}{2})$.

The Lagrange interpolation of a function on Chebyshev collocation points is closely related to an expansion of the function in terms of Chebyshev polynomials T_n , $n = 0, 1, \dots$

$$(15) \quad \tilde{v}(l) \approx \sum_{n=0}^N v_n T_n(l),$$

see the discussion in [22]. As shown again in [22], the Chebyshev coefficients v_n , $n = 0, 1, \dots, N$ can be computed efficiently via a fast cosine transform which is closely related to the fast Fourier transform. It is also known that the Chebyshev coefficients for a function analytic on $[-1, 1]$ decrease exponentially, and that the numerical error in approximating a function \tilde{v} via (15) is of the order of the first omitted coefficients v_n in the Chebyshev series.

3.4. Time integration. After the discretisation in space equation (13) becomes an $N + 1$ -dimensional system of ordinary differential equations (ODEs) in t of the form $\tilde{v}_t = f(\tilde{v})$ which can be numerically integrated in time with standard techniques. The discussion in [22] shows that Chebyshev differentiation matrices have a conditioning of the order $\text{cond}(D^3) = O(N^6)$. Thus explicit time integration schemes are problematic since stability conditions would necessitate prohibitively small time steps. Therefore, here we apply an implicit method, and since we are interested in capturing rapid oscillations in the expected DSWs, we use a fourth order method.

Concretely, we apply a fourth order Runge-Kutta (IRK4) scheme, also called the Hammer-Hollingsworth method, a 2-stage Gauss scheme. The general formulation of an s -stage Runge-Kutta method for the initial value problem $\tilde{v}' = f(\tilde{v}, t)$, $\tilde{v}(t_0) = \tilde{v}_0$ reads:

$$(16) \quad \tilde{v}_{n+1} = \tilde{v}_n + h \sum_{i=1}^s b_i K_i,$$

$$(17) \quad K_i = f \left(t_n + c_i h, \tilde{v}_n + h \sum_{j=1}^s a_{ij} K_j \right),$$

where b_i, a_{ij} , $i, j = 1, \dots, s$ are real numbers and $c_i = \sum_{j=1}^s a_{ij}$. For the IRK4 method used here, one has $c_1 = \frac{1}{2} - \frac{\sqrt{3}}{6}$, $c_2 = \frac{1}{2} + \frac{\sqrt{3}}{6}$, $a_{11} = a_{22} = 1/4$, $a_{12} = \frac{1}{4} - \frac{\sqrt{3}}{6}$, $a_{21} = \frac{1}{4} + \frac{\sqrt{3}}{6}$ and $b_1 = b_2 = 1/2$.

Applying IRK4 to (13) we get the following system,

$$(18) \quad \begin{aligned} \mathcal{L}K_1 &= -\frac{1}{1+l}[(1+l)(\tilde{v} + ha_{12}K_2) + V]_{xxx} \\ &\quad - \frac{1}{1+l}[(1+l)(\tilde{v} + ha_{11}K_1 + ha_{12}K_2) + V]^p[(1+l)(\tilde{v} + ha_{11}K_1 + ha_{12}K_2) + V]_x, \\ \mathcal{L}K_2 &= -\frac{1}{1+l}[(1+l)(\tilde{v} + ha_{21}K_1) + V]_{xxx} \\ &\quad - \frac{1}{1+l}[(1+l)(\tilde{v} + ha_{21}K_1 + ha_{22}K_2) + V]^p[(1+l)(\tilde{v} + ha_{21}K_1 + ha_{22}K_2) + V]_x, \end{aligned}$$

where

$$\mathcal{L} = \hat{1} + ha_{11} \frac{1}{1+l} \partial_{xxx}(1+l).$$

Recall that ∂_x is approximated in (18) via (14), and the third derivative with respect to x is approximated as the cubic power of this.

The system (18) will be solved iteratively with a simplified Newton iteration. This means that in each step of the iteration the new K_1 and K_2 are obtained by inverting the operator \mathcal{L} only instead of the full Jacobian. The vanishing boundary conditions for \tilde{v} and thus for K_1, K_2 are imposed as in [22]: the equations $\mathcal{L}K_i = F_i$, $i = 1, 2$, are solved by considering only the components $1, \dots, N-1$ of the K_i ; this means that we consider the reduced equations

$$\sum_{m=1}^{N-1} \mathcal{L}_{nm} K_{i,m} = F_{i,n}, \quad n = 0, \dots, N-1, \quad i = 1, 2,$$

and solve for $K_{i,1}, \dots, K_{i,N-1}$ only since the values $K_{i,0} = K_{i,N} = 0$ are imposed.

The resolution in time can be controlled via the conserved quantities of the generalised KdV equation. We consider in general the energy for functions vanishing at infinity. For functions which are just bounded at infinity, we consider a linear combination of the energy and the L^2 norm of the solution,

$$(19) \quad \tilde{E} = \int_{\mathbb{R}} \left(\frac{u^{p+1} - \lambda u^2}{p(p+1)} - \frac{1}{2} u_x^2 \right) dx,$$

where the constant λ is chosen such that the integrand is bounded at infinity. The conserved quantities will in actual computations depend on time due to numerical errors. But as discussed for instance in [14], the conservation of these quantities controls the numerical error which is in general overestimated by up to two orders of magnitude.

4. EXAMPLES

In this section we study two types of examples which illustrate the potential of the presented numerical approach. First we consider initial data in the form of a mollified (smoothed out) step function. Then we study initial data not satisfying the Faddeev condition $\int_{-\infty}^{+\infty} (1 + |x|)|u(x)|dx < \infty$, see [25], but nevertheless vanishing for $|x| \rightarrow \infty$. These examples are studied for two types of nonlinearity, for $p = 2$, the completely integrable KdV equation, and for $p = 4$, a non-integrable generalised KdV equation discussed for instance in [19]. The latter is still sub-critical which means that there is no blow-up for sufficiently regular initial data.

4.1. Mollified step initial data. We consider initial data of the form

$$(20) \quad u(x, 0) = \begin{cases} 1 & x < 0 \\ \exp(-x^{2n}) & x \geq 0 \end{cases},$$

where $n \in \mathbb{N}$. In Fig. 2 we show these data for $n = 4$ on the left, and the corresponding function \tilde{v} on the right (one has $A = -B = C = 1$).

Remark 4.1. The function (20) is analytic everywhere except at zero, where it is C^{2n-1} , thus the convergence rate of a spectral method is expected to be algebraic. Nevertheless, in practice this does not have a detrimental effect on our approach and, as we can see below in figure 4.1 on the right, the behavior of Chebyshev coefficients is, due to the finite precision used, virtually the same as in the analytic case.

For the time evolution of these data, we use $c = 2$, $N = 600$ and $N_t = 1000$ time steps for $t \in [0, 0.01]$. The resulting solution to the KdV equation can be seen in Fig. 3. The formation of a dispersive shock wave is clearly visible.

The slow decrease of the amplitude of the oscillations towards infinity, similar to the behaviour of the Airy function, is challenging for any numerical method. The Chebyshev coefficients v_n (15) of the solution are shown in Fig. 4, on the left for $t = 0$, on the right for $t = 0.01$. They decrease exponentially to the order of the rounding error for the initial data indicating that an analytic (within numerical precision, see remark 4.1) function is numerically well resolved. The algebraic decay of the spectral coefficients for $t = 0.01$ indicates an oscillatory singularity at infinity as for the Airy function. The spatial resolution is thus of the order of 10^{-4} . The relative conservation of the modified energy (19) is during the whole computation

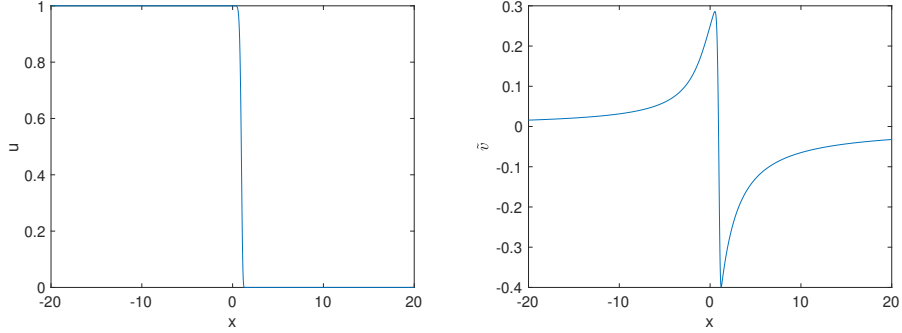


FIGURE 2. Initial data (20) for $n = 4$ on the left, and the corresponding $\tilde{v} = \tilde{v}(l(x))$ the right.

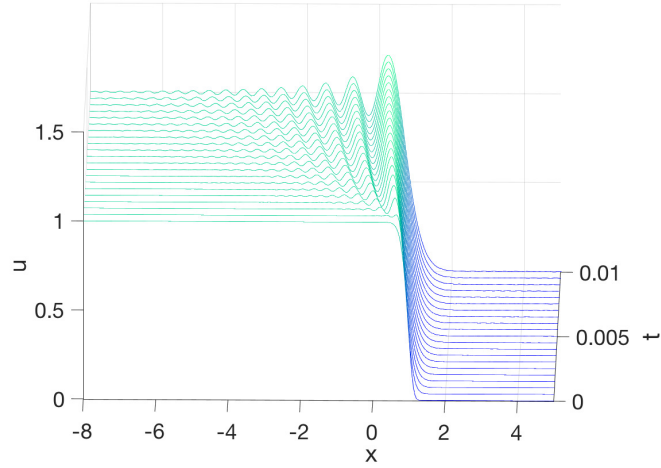


FIGURE 3. Solution to the KdV equation (1) with $p = 2$ for the initial data (20) for $n = 4$ in dependence of time.

of the order of 10^{-4} . This means the solution is obtained to better than plotting accuracy.

Note that the DSW is not the same as in the case of an exact step, the classical Gurevitch-Pitaevski problem [13]. But one can for instance verify that this is the correct solution by considering a finite step smoothed out at both sides,

$$(21) \quad u(x, 0) = \begin{cases} 1 & x_0 < x < 0 \\ \exp(-x^{2n}) & x \geq 0 \\ \exp(-(x - x_0)^{2n}) & x \leq x_0 \end{cases}$$

which can be conveniently treated with Fourier methods as in [14] to which the reader is referred for details and references. We use $N = 2^{12}$ Fourier modes for $x \in 10[-\pi, \pi]$ and $N_t = 1000$ time steps for a fourth order exponential time differencing

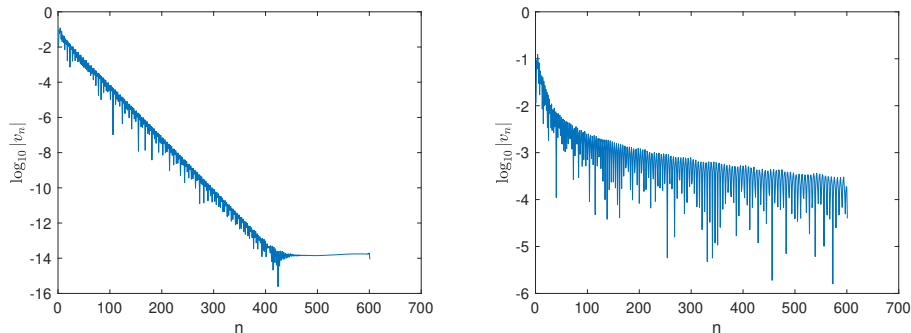


FIGURE 4. The Chebyshev coefficients (15), on the left for the mollified step initial data (20) on the right for the solution shown in Fig. 3 for $t = 0.01$

method. In Fig. 5 we show on the left the solution of Fig. 3 for $t = 0.01$, and for the initial data (21) with $n = 4$ and $x_0 = -5\pi$ at the same time.

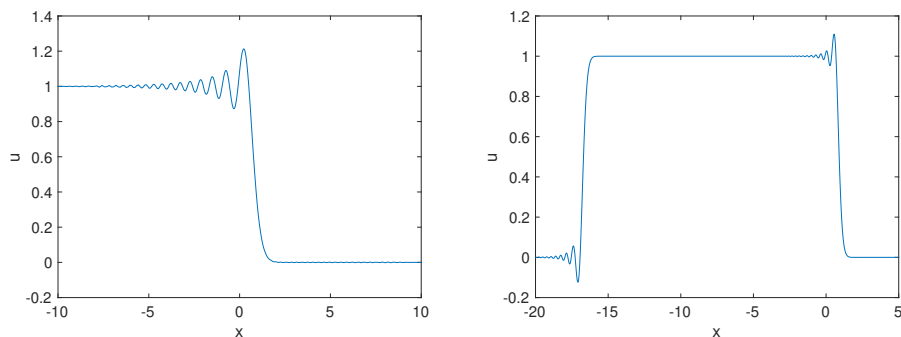


FIGURE 5. Solution to the KdV equation (1) with $p = 2$ for the initial data (20) on the left, and for the initial data (21) on the right, both for $n = 4$ and $t = 0.01$.

The solution to the generalised KdV equation with $p = 4$ for the same initial data as in Fig. 2 can be seen in Fig. 6. We have used the same numerical parameters as for the case $p = 2$, and we obtain the same numerical resolution. The form of the DSW is very similar to one for the standard KdV equation.

4.2. Slowly decaying initial data. In this subsection we consider initial data not satisfying the Faddeev condition, and we are interested in the long time behavior of the corresponding KdV solutions which is done by introducing a small parameter ϵ in (5). Concretely, we study initial data of the form

$$(22) \quad u(x, 0) = \frac{1}{(1+x^2)^a}, \quad a = \frac{1}{2}, 1.$$

We use $c = 2$, $N = 800$, and $N_t = 10^4$ time steps for $t \in [0, 10]$. In Fig. 7 we show the KdV solution ($p = 2$) in (5) for the initial data (22) for $\epsilon = 10^{-1}$ and $a = 1$ in dependence of time. It can be seen that several solitons appear.

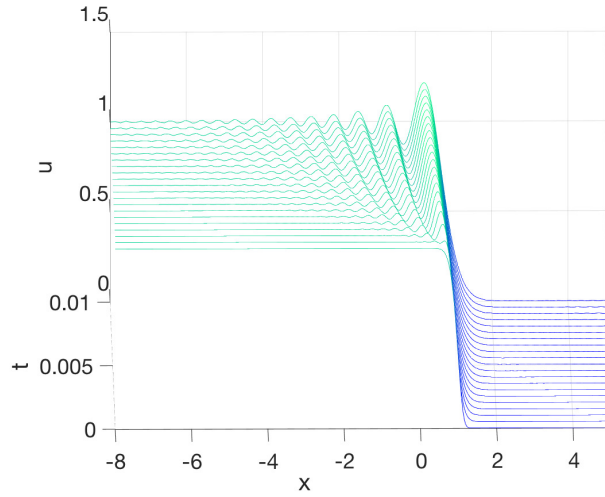


FIGURE 6. Solution to the generalised KdV equation (1) with $p = 4$ for the initial data (20) for $n = 4$ in dependence of time.

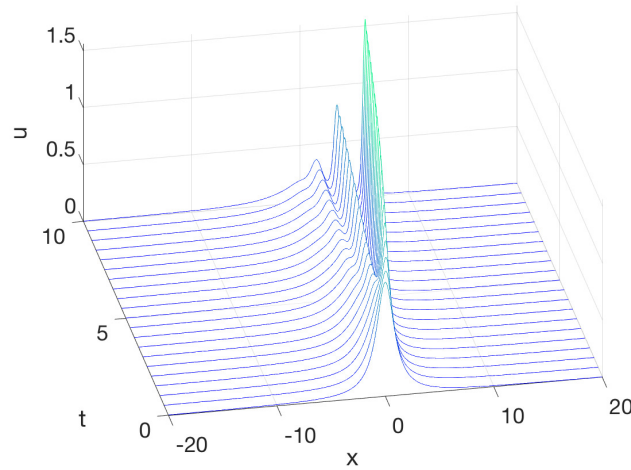


FIGURE 7. Solution to the KdV equation (1) with $p = 2$ for the initial data (22) for $a = 1$ in dependence of time.

The corresponding KdV solution for the initial data (22) with $a = 1/2$ and $\epsilon = 10^{-1}$ can be seen in Fig. 8. Note that in contrast to the case $a = 1$, the initial data do not satisfy the clamped boundary conditions for $x \rightarrow -\infty$, one has $A = -B = \pi/2$ and $C = 0$ in (11).

The solutions at the final time of Fig. 7 and 8 can be seen in Fig. 9, on the left for $a = 1/2$, on the right for $a = 1$. The slower decay towards infinity of the initial data with $a = 1/2$ can be recognized. But at the time $t = 10$, one observes the same number of solitons in both cases. The peaks in the solutions have been fitted to the solitons (4) which are shown in green in the same figure. It can be seen that

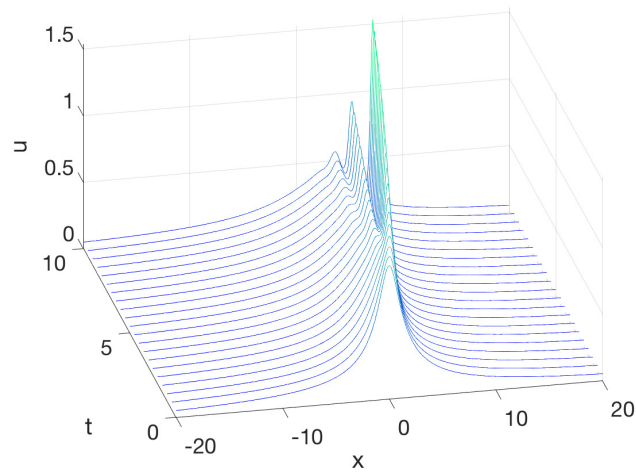


FIGURE 8. Solution to the KdV equation (1) with $p = 2$ for the initial data (22) for $a = 1/2$ in dependence of time.

the solitons are not yet fully separated from the background, but that they can be already clearly identified at this early stage.

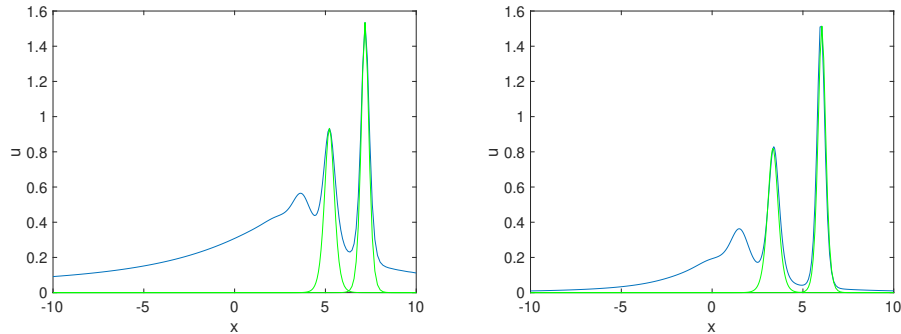


FIGURE 9. Solution to the KdV equation (1) with $p = 2$ for the initial data (22) for $t = 10$, on the left for $a = 1/2$, on the right for $a = 1$; in green fitted solitons (4).

The relative computed energy is in both cases conserved to the order of 10^{-10} . The Chebyshev coefficients for $t = 10$ are shown in Fig. 10, on the left for $a = 1/2$, on the right for $a = 1$. It can be seen that the coefficients decrease as expected exponentially, and that the solutions are well resolved in space as well.

If the same initial data as in Fig. 9 are considered for the generalised KdV equation (5) with $p = 4$, one obtains for $t = 10$ the solutions shown in Fig. 11. The solitons are here much more peaked than in the KdV case of Fig. 9 which is also illustrated by the fit to the solitons. Consequently the same numerical parameters as there lead for the generalised KdV solution to a lower resolution:

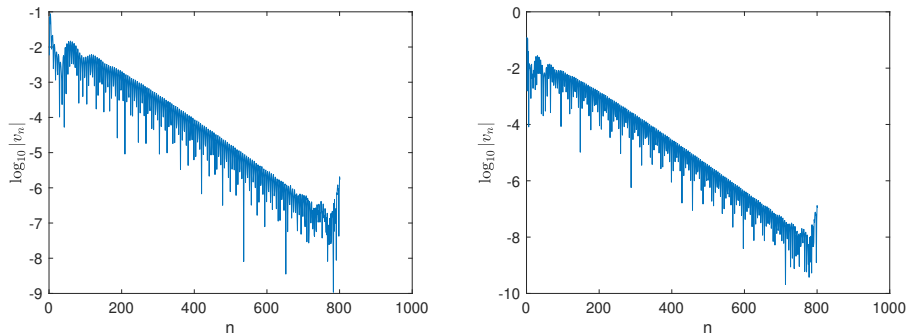


FIGURE 10. Solution to the KdV equation (1) with $p = 2$ for the initial data (22) for $t = 10$, on the left for $a = 1/2$, on the right for $a = 1$.

the relative conservation of the energy is of the order of 10^{-4} , and Chebyshev coefficients decrease still exponentially, but only to the order of 10^{-6} in this case.

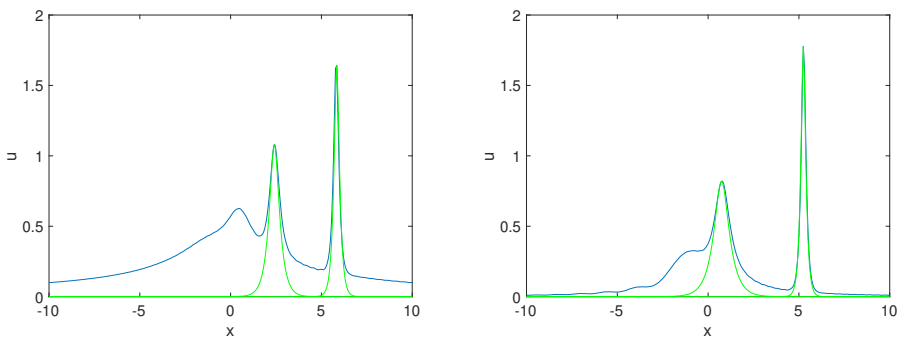


FIGURE 11. Solution to the KdV equation (1) with $p = 4$ for the initial data (22) for $t = 10$, on the left for $a = 1/2$, on the right for $a = 1$.

5. OUTLOOK

In this paper we have presented a numerical approach for generalised KdV equations on the compactified real line which allows to approximate functions which are smooth on $\mathbb{R} \cup \{\infty\}$ with spectral accuracy, i.e., with a numerical error decreasing exponentially with the number of collocation points. The time integration is performed with an implicit fourth order method. One direction of further research will be to improve the efficiency of the time integration, ideally an explicit approach, for instance similar to the approach of [16] in the context of the Schrödinger equation.

Of special interest is, however, the application of the techniques of the present paper to the numerical study of blow-up in the context of generalised KdV equations, i.e., for (1) with $p \geq 5$. The current approach would allow to study the dynamically rescaled generalised KdV equations, see for instance [15] without the problems there related to the use of Fourier methods. In this context it would be

beneficial to apply a multidomain spectral method as in [3] for Schrödinger equations where the compactified real axis is divided into several domains each of which is mapped to the interval $[-1, 1]$. This allows for a more efficient allocation of numerical resolution than via the choice of the parameter c in (7), in particular a higher resolution near the expected blow-up. To this end, matching conditions at the domain boundaries (the solution u has to be C^2 there) have to be imposed which is numerically problematic. This will be a subject of further research.

REFERENCES

- [1] Belokolos E, Bobenko A, Enolskii V, Its A and Matveev V 1994 *Algebro-Geometric Approach to Nonlinear Integrable Equations*, Springer Series in Nonlinear Dynamics (Berlin: Springer)
- [2] J. Bérenger. A perfectly matched layer for the absorption of electromagnetic waves. *J. Comput. Phys.* 114, 185-200, 1994.
- [3] M. Birem and C. Klein, Multidomain spectral method for Schrödinger equations, *Adv. Comp. Math.*, 42(2), 395-423 DOI 10.1007/s10444-015-9429-9 (2016)
- [4] J. L. Bona, P. E. Souganidis, W. A. Strauss, Stability and instability of solitary waves of Korteweg-de Vries type, *Proc. R. Soc. Lond. A* 411 (1987) 395 - 412.
- [5] B. Dubrovin, On Hamiltonian perturbations of hyperbolic systems of conservation laws, II: universality of critical behaviour, *Comm. Math. Phys.* 267 (2006) 117 - 139.
- [6] B. Dubrovin, On universality of critical behaviour in Hamiltonian PDEs, *Amer. Math. Soc. Transl.* 224 (2008) 59-109.
- [7] B. Dubrovin, T. Grava and C. Klein, Numerical Study of breakup in generalised Korteweg-de Vries and Kawahara equations, *SIAM J. Appl. Math.*, Vol 71, 983-1008 (2011).
- [8] L.D. Faddeev, On the relation between the S-matrix and potential for the one dimensional Schrödinger operator, *Dok. Akad.Nauk SSSR* 121 (1958), 63-66, see also *Amer. Math. Soc. Transl.* (2) 65 (1967), 139-166.
- [9] A.S. Fokas: The generalised Dirichlet-to-Neumann map for certain non linear evolution PDEs. *Comm. Pure Appl. Math.* 58(5), 639-670 (2005)
- [10] T. Grava and C. Klein, Numerical study of the small dispersion limit of the Korteweg-de Vries equation and asymptotic solutions, *Physica D*, 10.1016/j.physd.2012.04.001 (2012).
- [11] T. Grava, A. Kapaev, and C. Klein, On the tritonquée solutions of P_I^2 , *Constr. Approx.* 41, 425 -466, DOI 10.1007/s00365-015-9285-3 (2015).
- [12] C.E. Grosch and S.A. Orszag, Numerical solution of problems in unbounded regions: coordinate transforms, *J. Comput. Phys.* 25, 273-296 (1977).
- [13] A. V. Gurevich, L. P. Pitaevskii, Nonstationary structure of a collisionless shock wave. *Eksper. Teoret. Fiz.* 65 (1973), no. 8, 5901-7604; translation in *Soviet Physics JETP* 38 (1974), no. 2, 2911-7297.
- [14] C. Klein, Fourth order time-stepping for low dispersion Korteweg-de Vries and nonlinear Schrödinger equation, *ETNA* Vol. 29 116-135 (2008).
- [15] C. Klein and R. Peter, Numerical study of blow-up in solutions to generalised Korteweg-de Vries equations, *Physica D* 304-305 (2015), 52-78 DOI 10.1016/j.physd.2015.04.003.
- [16] C. Klein, N. Stoilov, Numerical study of the transverse stability of the Peregrine solution, *Stud Appl Math.* 145 (2020) 36-51. <https://doi.org/10.1111/sapm.12306>
- [17] V.A. Marchenko, *Sturm-Liouville operators and applications*. Revised edition, AMS Chelsea Publishing vol. 373 (2001).
- [18] Y. Martel and F. Merle, Stability of Blow-Up Profile and Lower Bounds for Blow-Up Rate for the Critical generalised KdV Equation, *Ann. Math.*, 155, (2002), 235-280.
- [19] Y. Martel, F. Merle, On the nonexistence of pure multi-solitons for the quartic gKdV equation. *Int Math Res Notices* (2015) (3): 688-739.
- [20] Y. Martel, F. Merle, P. Raphaél, Blow up for the critical gKdV equation I: dynamics near the soliton. *Acta Math.* 212 (2014), no. 1, 59-140.
- [21] T. L. Perel'man, A. Kh. Fridman, and M. M. El'yashevich, A modified Korteweg-de Vries equation in electrohydrodynamics, *Sov. Phys. JETP*, Vol. 39, No.4, October 1974
- [22] L.N. Trefethen, *Spectral Methods in Matlab*, SIAM, Philadelphia, PA (2000)
- [23] www.comlab.ox.ac.uk/oucl/work/nick.trefethen

- [24] J.A.C. Weideman, S.C. Reddy: A Matlab differentiation matrix suite. ACM TOMS 26, 465-1-7519 (2000)
- [25] V.E. Zakharov ed., . *What is integrability?*. Berlin: Springer-Verlag, (1991).
- [26] C. Zheng, A perfectly matched layer approach to the nonlinear Schrödinger wave equations. J. Comput. Phys. 227, 537-556 (2007)
- [27] C. Zheng, Numerical simulation of a modified KdV equation on the whole real axis, Numer. Math. (2006) 105:315-335 DOI 10.1007/s00211-006-0044-z

INSTITUT DE MATHÉMATIQUES DE BOURGOGNE, UMR 5584, UNIVERSITÉ DE BOURGOGNE-FRANCHE-COMTÉ, 9 AVENUE ALAIN SAVARY, 21078 DIJON CEDEX, FRANCE, E-MAIL CHRISTIAN.KLEIN@U-BOURGOGNE.FR

INSTITUT DE MATHÉMATIQUES DE BOURGOGNE, UMR 5584, UNIVERSITÉ DE BOURGOGNE-FRANCHE-COMTÉ, 9 AVENUE ALAIN SAVARY, 21078 DIJON CEDEX, FRANCE, E-MAIL NIKOLA.STOILOV@U-BOURGOGNE.FR